International Journal of Integrated Sciences & Technology **4** S (2022) 14-25

International Journal of Integrated Sciences & Technology (IJIST)
http://www.cuet.ac.bd/IJIST/index.html

A Comparative Numerical Study of High-Efficiency Lead Halide and Tin Halide Perovskite Solar Cell Based on Different Hole Transport Materials

Monjur M. Rabby[1]*, Mounita Ghosh[2], S. Z. Ali[1], Kazi S. Nowaz[3]

[1]*Bangladesh University of Engineering and Technology, Dhaka, Bangladesh*

[2]*Bangbabandhu Sheikh Mujibur Rahman Science & Technology University, Bangladesh*

[3]*Rajshahi University of Engineering and Technology, Rajshahi, Bangladesh*

ABSTRACT

Tin and lead halide perovskite solar cell have been designed and simulated using Solar Cell Capacitance Simulator (SCAPS) with three different hole transport materials (HTM) such as: Copper Iodide (CuI), poly (3,4-ethylene dioxythiophene) polystyrene sulfonate (PEDOT: PSS) and Spiro-OmeTAD. Titanium Oxide was used as an electron transportation materials (ETM) and ZnO as a conductive oxide layer. The tin halide perovskite exhibited better efficiency than that of lead halide perovskite with same layer of HTM and ETM parameters. The open-circuit voltage was noted to be increased with the decrease of absorber layer's thickness and reverse for the short circuit current. It has also been observed that the performance of the solar cell changed with the variation of HTM's thicknesses. A drastic change was been observed in performance of the solar cell for varying thickness of PEDOT: PSS layer after a certain thickness.

Keywords: Perovskite, Solar cell, SCAPS, Thickness, Efficiency.

1. Introduction

Perovskites are a class of materials that share a resembling structure and display an innumerable number of unique properties such as, magneto-resistance, superconductivity and many more. The optoelectronic behavior, high power conversion efficiency and low manufacturing cost of organometal halide perovskite solar cells have recently enticed significant interest from scientific community [1]. Among them, lead-halide ($CH_3NH_3PbX_3$, X = Cl, Br, I) perovskite solar cells (PSCs) are leading the race because of their lower cost and simpler processing techniques compared to silicon based conventional solar cells [2]. Though these materials are cost-effective, their instability, toxicity (due to the presence of lead) are considered as their lacking [3]. The most efficient perovskite solar contains lead (Pb) but to confront the disadvantages mentioned earlier, tin (Sn) is being considered as the most feasible substitute [4].Replacement of Pb^{2+} by Sn^{2+} as well as Sr^{2+}, Ca^{2+} and Cd^{2+} in these perovskites solar cell have been experimented both theoretically and experimentally lately [5].

In this research work, Solar Cell Capacitance Simulator (SCAPS) has been used to simulate solar cells with different parameters that are mentioned in the following paragraph. It is a device simulator which is used to simulate solar cells is a one-dimensional solar cell simulation program that flourished at the department of Electronics and Information Systems (ELIS) of the University of Gent, Belgium. Several researchers Alex Niemegeers, Marc Burgelman, Koen Decock, Johan Verschraegen, StefaanDegrave have contributed considerably to develop SCAPS [6]. Toxicity of lead-based perovskite solar cells can be confronted by using $CH_3NH_3SnI_3$with a band gap of 1.30 eV as an absorber layer. Among the $CH_3NH_3BX_3$ (B=Sn, Pb; X=Cl, Br, I) compounds, it ($CH_3NH_3SnI_3$) has the most appropriate optical properties that provides good light-absorption range for optoelectrical applications [7]. In typical perovskite solar cells, TiO_2 is used as the ETM layer which causes unstable charge transport of perovskite solar cells. To achieve high performance, long-term stability and robust production with improved potency, coating of titanium oxide (TiO_2) is primarily used. Moreover, in recent studies, ZnO has been used as a suitable replacement for TiO_2 without significantly affecting PSC's output [8-10]. On the other hand as HTM, Copper Iodide (CuI) as a p-type transparent conducting thin film, provides the most desirable properties. CuI films exhibit some excellent qualities such as high conductivity, wide-bandgap, good stability and they are hydrophobic. Recently Spirobifluorene (spiro-MeOTAD) hole transport material (HTM) has become a landmark in the

Corresponding author:
E-mail: rabbymorshed@gmail.com
For color version visit: http://www.cuet.ac.bd/IJIST/index.html

ISSN: 2411-9997

history of perovskite solar cells (PSCs) due to their efficient charge extraction capability [11-15]. Spiro-MeOTAD mainly consists of 4-tert-butylpyridine and bis (trifluoromethane) sulfonamide lithium salt. However, the dissolving nature of 4-tert-butylpyridine in the perovskite absorber layer and the destruction of the perovskite layer by bis (trifluoromethane) sulfonamide lithium salt through the oxidation process is considered as the main problem in this case [16-17]. Though Poly (3,4-ethylenedioxythiophene) - poly (styrenesulfonate) (PEDOT: PSS) has poor stability and hygroscopic nature that affects the solar cell performance, but it is playing a promising role in (HTL) nowadays[18]. Correa-Baena and Hagfeldt obtained an efficiency of 21.9% for perovskite solar cell [19]. In 2016, Wolfgang Tress has achieved photo-voltages of >1.2 V in inorganic-organic lead-halide perovskite solar cells within a few years of research [20]. Perovskite materialshave huge advantages like long diffusion length and long minority carrier lifetimes. Due to the light-weighted features, high efficiencies (over 20%) and low-cost production, it has some promising applications these days. But it has also some drawbacks like poor thermal stability, poor stability to moisture, operational instability and most importantly toxicity. In this paper, using SCAPS-1D, device simulations have been done for Glass / ZnO / TiO_2 / $CH_3NH_3SnI_3$ / HTM / Au and Glass / ZnO / TiO_2 / $CH_3NH_3PbI_3$ / HTM / Au structure. In order to monitor their efficiency, different types of layers of HTM both organic and inorganic have been used. The aim is to observe how the performance shifts while substituting lead by tin-based perovskite under the same working environment and also to get an insight into the working principle of perovskite-structure materials based on their electrical parameters. It was observed that the open-circuit voltage increased as the thickness of the absorber decreased, vice versa for short circuit current. The performance of the solar cell changed with varying thickness of HTM. A drastic change was observed in performance for varying thickness of Spiro-OmeTAD layer in tin halide PSC. Finally, we tried to develop an empirical equation that can predict the efficiency in respect of varying thickness of absorber and HTM layer. Researchers who work on perovskite solar cells with different HTM layers may use this function to get an approximate idea about the efficiency with varying thicknesses of both absorber and hole transport layer in a standard condition.

2. Materials and Methods

Here, SCAPS-1D software was used to design and simulate halide-based perovskite solar cells. This software works based on some basic equations such as the Poisson equation and the continuity equations [7]. The poison equation relates the electrostatic potential to charge distribution which is mainly used to determine the electrostatic field by describing the potential field caused by charge distribution. The poison equation can be written as follows:

$$\frac{\partial^2}{\partial x^2}\psi(x) = -\frac{q}{\epsilon}(p - n + C) \qquad (1)$$

$$C = (N_D - N_A) + (P_P - P_n) \qquad (2)$$

Here, ϵ = Dielectric constant, Ψ= Electrical potential, q= amount of charge p= hole density, n=electron density. Here, N_D and N_A represent the defect concentration of donor and acceptor, respectively. Besides, p_p and p_n represent the concentration of trapped holes and electrons. The generation and recombination of charge can be described by the continuity equation.

$$-\frac{1}{q}\frac{\partial J_n}{\partial x} = G_n - R_n \qquad (3)$$

$$\frac{1}{q}\frac{\partial J_p}{\partial x} = G_p - R_p \qquad (4)$$

Where G= rate of carrier generation, R= rate of recombination of electrons and holes.

If it is found a positive value that means recombination occurs, however, a negative value means the generation of carriers. Based on the electrical and optical properties of materials, it can simulate efficiency and other electrical characteristics and spectral response of the designed solar cells. This simulation software helps us to get an estimated idea over the change of a wide range of different parameters of materials. Moreover, the different working environments can be simulated under which solar cell works. The parasitic resistances can be controlled which are part of the solar cell circuit, which can also affect solar cell efficiency. In this simulation, a one-dimension structure layer with an architecture of hole transport layer, perovskite absorber layer, electron absorber layer and conductive oxide layer has been designed. As a hole transport layer, three different materials such as Copper Iodide (CuI), poly (3,4ethylene dioxythiophene) polystyrene sulfonate (PEDOT: PSS), and Spiro-OmeTAD has been chosen. PEDOT: PSS is a conducting polymer that is made up of two ionomers. CuI is an inorganic material, while Spiro-OmeTAD is an organic compound. The main component of our designed solar is the perovskite layer. We used both Methylammonium lead halide and Methyl ammonium tin halide layer as an absorber and make a comparison of their performance. Their stability can be measured by the tolerance factor (t) from the Goldschmidt equation-

ISSN: 2411-9997

$$t = \frac{r_a + r_b}{\sqrt{2}(r_b + r_0)} \qquad (5)$$

For most stable perovskite materials, the tolerance factor is in the range of 0.8 to 1. An ideal type of perovskite with a cubic crystal structure is found at a tolerance factor of 1. For 0.9 <t <1.0, the perovskites with a cubic crystal structure are formed. The distorted perovskite structures such as orthorhombic, tetragonal, crystal structures are likely to be formed when the tolerance factor is between 0.80 to 0.89 [22].$MAPbI_3$ (t=0.9) is believed to be the most stable one so far. The calculated tolerance factor of $MASnI_3$ is 0.94. However, factors such as temperature, pressure and ion radius can cause a phase transition of $MAPbI_3$ from cubic to tetragonal structure. Also, the presence of moisture, air, and high-energy photon can decompose the perovskite layer. The conventional Titanium oxide as an electron transport layer has been used which shows an energy bandgap favorable to perovskite structured solar cells. Titanium oxide also provides good electron mobility and allows long electron life. Here zinc oxide was used as conducting transport layer, sometimes titanium oxide can be replaced with zinc oxide. Zinc oxide is very useful as a conducting layer for its high charge carrier mobility. By using ZnO, the thickness of the titanium oxide layer can be reduced. Generally, Al-doped ZnO can be used as ETL material to reduce the cost of fabrication. However, Al-doped ZnO causes rapid thermal decomposition of the Perovskite layer. Therefore, for better stability, we used an optimum layer of TiO_2 layer with ZnO conducting layer. The structure assumes to be placed on a glass substrate.The material parameters used in the modeling and simulation of this solar cell were derived from literature and experimental values. In some cases, logical and reasonable estimates were considered where precise experimental values are not available as shown in table 1. The performance of solar cells was measured at 300K temperature. The solar cell was illuminated with light incident power 1000 w/m^2, and the spectrum simulation was done considering an air mass of 1.5 at one sun. During the simulation, the absorption coefficient was considered $1\times10^5 cm^{-1}$ and background absorption was assumed 1.00 cm^{-1}. For the perovskite layer, the Auger electron and hole capture coefficient were 1×10^{-29} cm^6/s. The radiative recombination coefficient was considered $3.0\times10^{-11} cm^3/s$ from the literature [27]. The sum of the radiative recombination rates, Auger recombination rates, and SRH recombination rates gives the bulk lifetime of the carrier.

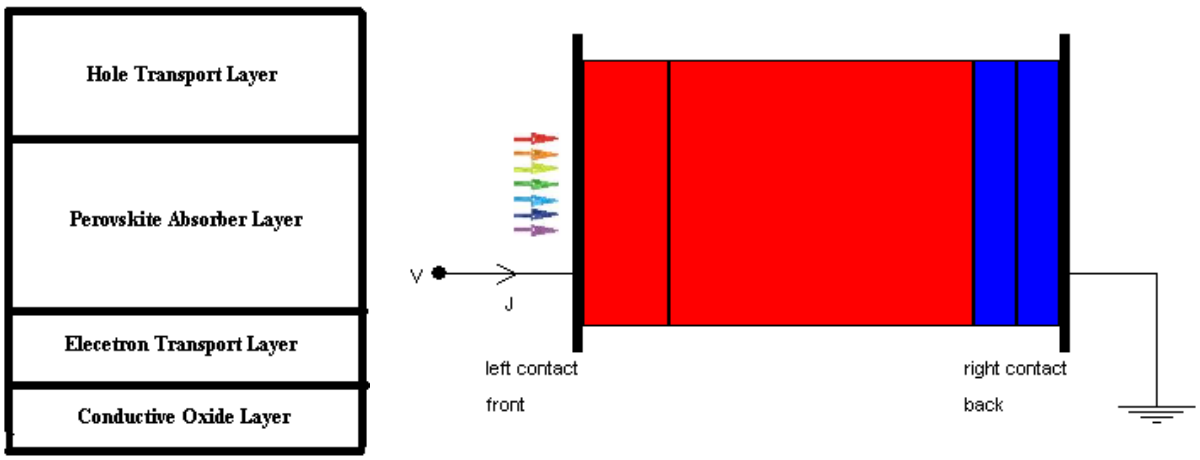

Fig. 1: Schematic diagram of Perovskite Solar cell

Table 1: Simulation device materials parameters [23, 24, 25, 26].

Parameter	$CH_3NH_3PbI_3$	$CH_3NH_3SnI_3$	TiO_2	ZnO	CuI	PEDOT : PSS	Spiro-OmeTAD	PCBM
Thickness	variable	variable	variable	variable	variable	variable	variable	.05
Band gap (eV)	1.480	1.300	3.260	3.470	3.100	3.200	3.000	1.30
Electron Affinity (eV)	3.930	4.170	4.200	4.300	2.100	2.450	2.450	4

ISSN: 2411-9997

Dielectric Permittivity, E	18.000	6.500	10.000	9.000	6.500	3.000	3.000	9.00
Conduction band effective density of states ($1/cm^3$)	3.200E+18	1.000E+18	2.200E+18	2.000E+18	2.200E+19	2.200E+18	2.500E+18	1.500E+18
Valance band effective density of states ($1/cm^3$)	5.000E+19	1.000E+19	1.800E+19	1.800E+20	1.800E+19	1.800E+19	1.800E+19	1.800E+19
Electron thermal velocity (cm/s)	1.000E+7	1.000E+6	1.000E+7	1.000E+7	1.000E+7	1.000E+7	1.000E+7	1.000E+7
Hole thermal velocity (cm/s)	1.000E+7	1.000E+6	1.000E+7	1.000E+7	1.000E+7	1.000E+7	1.00E+7	1.000E+7
Electron mobility (cm^2/Vs)	2.000E+0	1.600E+0	1.00E+2	1.000E+2	1.000E+2	5.000E-4	2.000E-4	2.000E-3
Hole mobility (cm^2/Vs)	2.000E+0	1.600E+0	2.500E+1	2.500E+1	4.390E+1	5.000E-4	2.000E-4	2.000E-4
Donor density ($1/cm^3$)	0	0	1.000E+18	1.000E+19	0	0	0	5.000E+18
Acceptor density ($1/cm^3$)	1.000E+13	3.200E+15	0	0	1.000E+18	1.000E+19	1.000E+18	0
Defect Density ($1/cm^3$)	1.000E+14	1.000E+16	0	1.000E+14	0	0	1.000E+14	1.000E+16

Here, Au (metalwork function=5.45eV) is served as front contact and flat bands set up were used for back contact. The thermionic emission velocity for electron and hole was maintained 1×10^5cm/s and 1×10^7cm/s, respectively. The Schematic diagram of the Perovskite Solar cell shows the direction of the applied voltage. A test simulation was performed to validate our simulated result with Shuang Sun's experimental data [28]. We simulated an structure of ITO (150 nm) / PEDOT:PSS (50 nm) / $MAPbI_3$ (50 nm) / PCBM (50 nm) / Al. The simulation results showed a close agreement with the experimental data. The same parameter was used in this simulation.

Table 2: Comparison between Experimental and Simulation result

Parameters	Voc (V)	Jsc (mA/cm2)	Fill factor (%)	Efficiency (%)
Experimental	0.82	8.2	77.00	5.20
Simulation	0.82	7.40	70.86	4.34

3. Results and Discussion

The maximum efficiency for both tin and lead halide perovskite absorber layer has been obtained using an optimal thickness of 500nm and 400nm of HTML. With this optimum thickness, both tin and lead halide-based perovskite solar cells were simulated to find out their maximum efficiency and favorable open-circuit voltage. The lead-based perovskite solar cell having PEDOT: PSS as the hole transport layer showed a maximum efficiency of 13.07% with optimum open-circuit voltage, V_{oc}= 1.0535V. Furthermore, for CuI and Spiro-OmeTAD layers, we obtained an efficiency of

ISSN: 2411-9997

12.63% and 12.78% respectively. In 2015, Sang Hyuk showed in his experiment that PEDOT: PSS based lead-based PSCs could achieve the best PCE of 18.1% [29].

Table 3: Simulation results of lead halide perovskite solar cell with different HTM layer

HTM layer	Voc (V)	Jsc (mA/cm^2)	Fill factor (%)	Efficiency (%) (including series and shunt resistant)	Efficiency (%) (without series and shunt resistance)
PEDOT:PSS	1.0535	21.98	49.59	13.07	16.79
CuI	0.9863	24.14	54.61	13.01	15.78
Spiro-OmeTAD	1.0251	23.51	53.03	12.78	15.83

Mansoo Choi and Nam-Gyu Park observed in their experiment that Spiro-MeoTAD based lead halide PSCs reveal PCE ranging from 6% to 19.7% [30]. Junyou Yang and Qinghui Jiang investigated that when CuI film was prepared by facile spray deposition, PCE reached up to 17.6% for $CH_3NH_3PbI_3$ solar cell [31]. During the simulation, to create an environment of real practice series and shunt resistance of 4.25ohm.cm^2 and 500ohm.cm^2 has been considered, respectively. The series and shunt resistance of the solar cell circuits affect the efficiency of the solar cells. Therefore, a solar cell without a series and shunt resistance has been simulated. The maximum efficiency was achieved by 16.79% for lead halide PSc and 22.97% for tin halide PSc when series and shunt resistance were neglected. However, the tin-based perovskite solar cell including PEDOT: PSS as the hole transport layer, showed the highest efficiency of 18.36% and V_{oc} =1.34V for optimum parameters. Moreover, for CuI and Spiro-OmeTAD layers, the tin-based perovskite solar cell offered an efficiency of 16.94% and 17.71% respectively. The simulation result for tin halide perovskite showed a close agreement with simulation results from the literature. Hi Jing et al showed in their simulation that tin halide PSC can achieve PCE in the range of 16.50% to 23.36%. Farhanaet al also observed closely similar PCE for tin halide PSC.

Table 4: Simulation results of tin halide perovskite solar cell with different HTM layer

HTM layer	V_{oc} (V)	Jsc (mA/cm2)	Fill factor (%)	Efficiency (%) (including series and shunt resistant)	Efficiency (%) (without series and shunt resistant)
PEDOT:PSS	1.3401	31.65	43.27	18.36	22.97
CuI	1.1380	31.52	47.23	16.94	20.91
Spiro-OmeTAD	1.1565	31.27	48.95	17.71	21.99

Their simulation showed PCE in the range of 18.34% to 20.23% [24-25]. At maximum irradiance, lead halide PSC with CuI layer showed a current density of 24.14mA/cm^2.On the other hand, at maximum irradiance tin halide PSC with PEDOT: PSS layer showed a maximum current density of 31.65mA/cm^2. The series R_s and shunt resistance R_{sh} reduce the current density to a certain extent. These resistances also affect the fill factor. Series resistance, R_s, includes physical resistance of the semiconductor layers and that of the front and back contacts. Shunt resistance, R_{sh}, can be described as leakage current around the edge of the cell. The solar cell works as a current generator. A single diode-based circuit can be assumed for solar cells with two parasitic resistances. The incident photons create electron-hole pairs. A forward bias voltage is generated by the photovoltaic effect of the solar cell and applied to the diode. The current generated in a solar cell is diverted into a forward-biased diode and the rest of the current leads to the external circuit.

$$I = I_{photon} - I_o \left(exp \frac{q(V+IR_S)}{aKt} - 1 \right) - \frac{(V+IR_s)}{R_{sh}} \qquad (6)$$

ISSN: 2411-9997

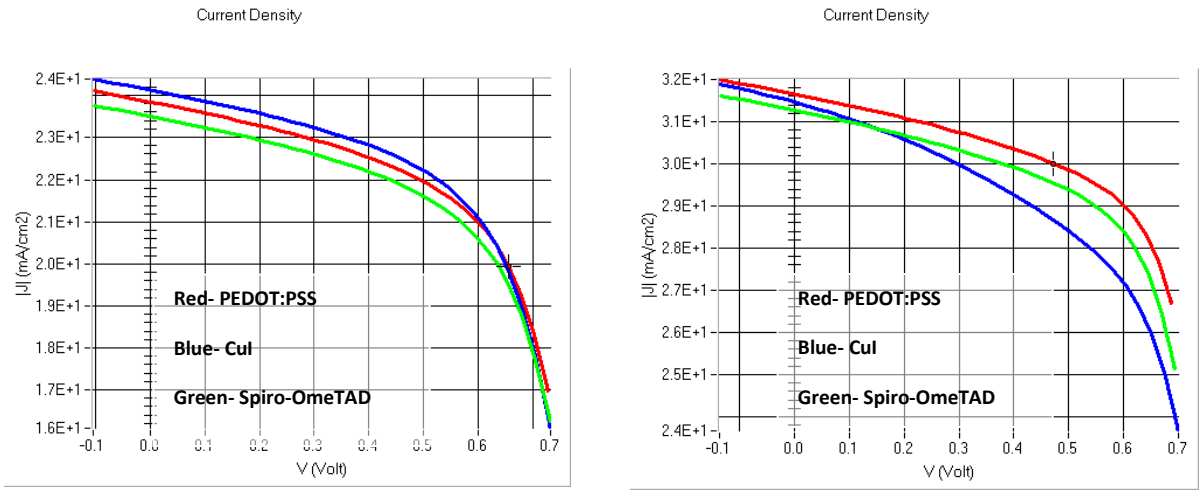

a) b)

Fig. 2: J-V curves for a) lead halide PSC & b) tin halide PSC with different HTM layer

The final current can be written as equation 6. J-V characteristic graph is plotted from this equation. Fig 2 showed the J-V curve where the blue line represents PEDOT:PSS, the red line indicates CuI and the green line for Spiro-OmeTAD.From fig 3 it is clearly observed that the tin halide perovskite showed better efficiency and better open-circuit voltage than lead halide PSC. Among all three HTM layers, PEDOT: PSS and Spiro-OmeTAd are the promising hole transport layers. However, CuI also showed very decent efficiency and favorable open-circuit voltage. Copper Iodide is an inorganic compound, and its stability is better than the others [25]. The variation in thickness of the perovskite layer can affect the efficiency of solar cells. It has been observed how variation in thickness of perovskite layer responses with different HTM layer.

(a)

(b)

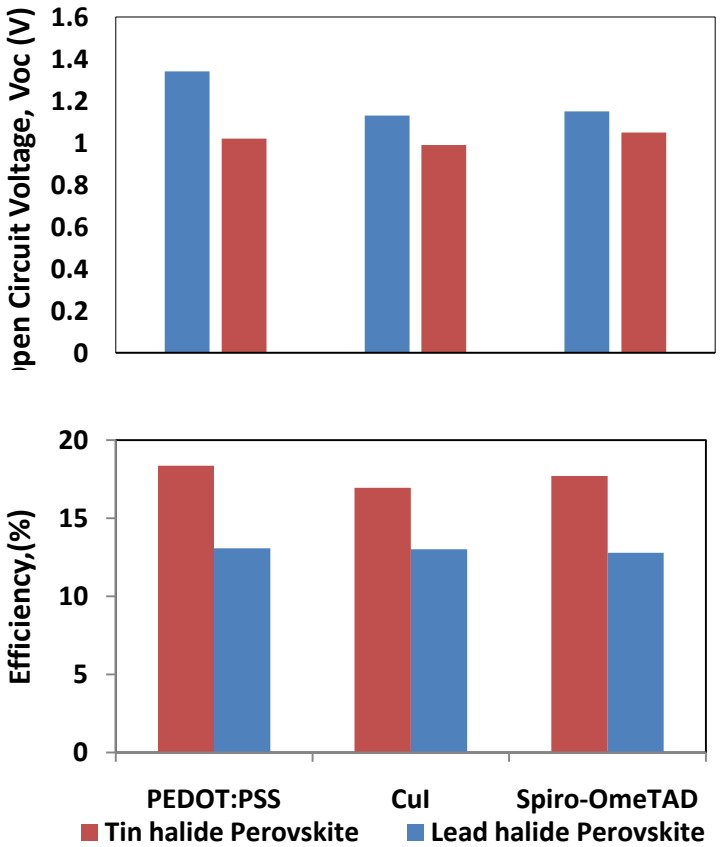

Fig. 3: Comparative analysis of a) efficiency and b) open circuit voltage between lead halide and tin halide PVs

ISSN: 2411-9997

Here, the thickness was varied from 300nm to 1000nm. During simulation, HTM layer thickness was maintained at 200nm and the thickness of the ETM layer was kept at 100nm. From this observation, we found an optimum thickness of 400nm and 500nm for lead and tin halide PSC respectively which is mentioned before. For both lead and tin halide PSC, the efficiency decreases in the same pattern after the optimum thickness. A slight change was observed in open-circuit voltage with varying thickness of absorber. The graph indicates that open-circuit voltage slightly increased with decreasing thickness of the absorber layer. However, the tin halide PSC with PEDOT: PSS layer showed a drastic variation in open circuit voltage with varying thickness.

(a)

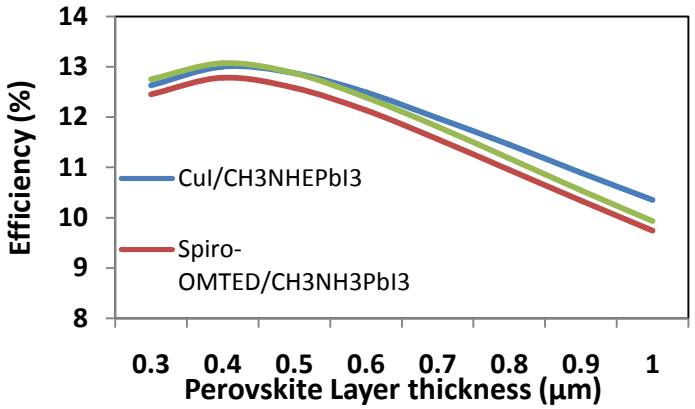

(b)

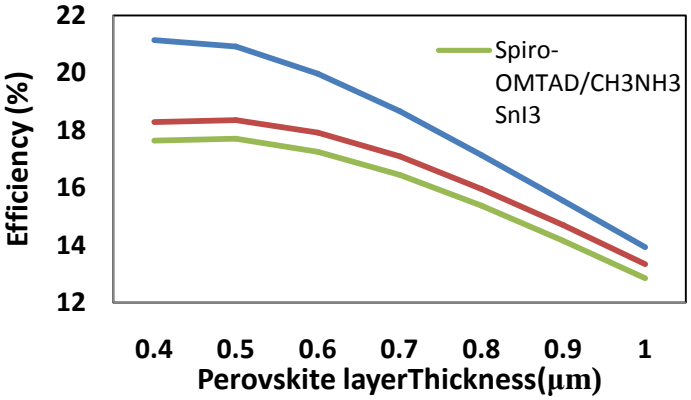

Fig. 4: Efficiency of a) Lead halide PVs b) Tin halide PVs with different HTM layer and with varying thickness of absorber.

The simulated result showed that the open-circuit voltage of 1.42V can be achieved at 400nm thickness of absorber layer, however, maximum efficiency cannot be obtained at this thickness. Usha Mandadapu et al performed a simulation to investigate the variation of solar cell parameters with the band gap (eV) of the absorber layer, and at that time he found open circuit voltage of above 1.36V for tin halide perovskite layer [32].

ISSN: 2411-9997

(a)

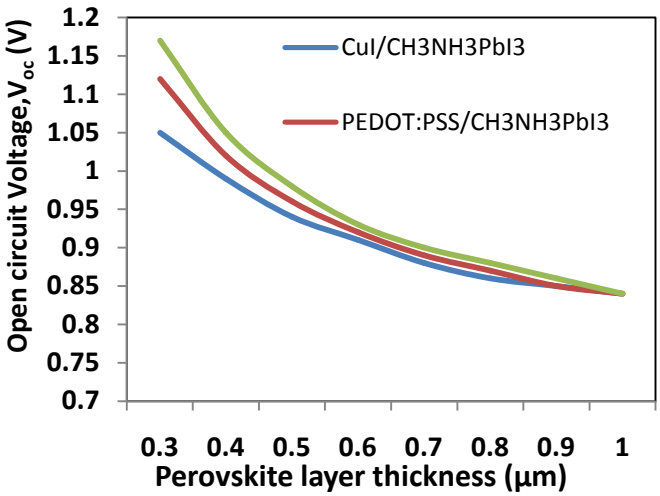

(b)

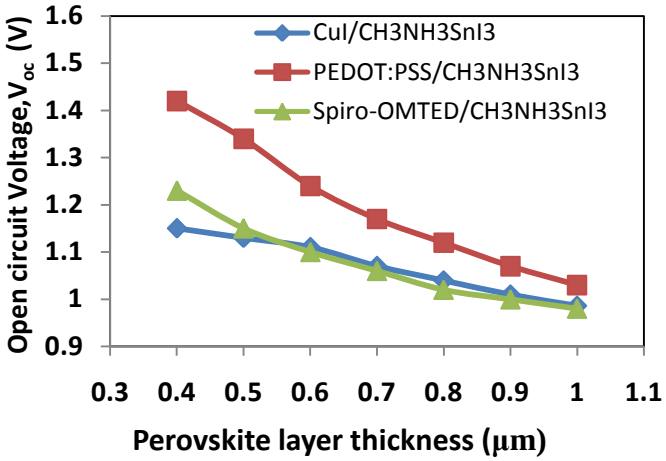

Fig. 5: Open circuit voltage of a) Lead halide PVs b) Tin halide PVs with different HTM layer and with varying thickness of absorber.

In lead halide perovskite solar cell, the short circuit current increases with the increased thickness of the absorber layer though the change occurs to a very small extent. However, in tin halide perovskite solar cell, a peak has been observed at which maximum Isc was found. For CuI/$CH_3NH_3SnI_3$and PEDOT: PSS/$CH_3NH_3SnI_3$, maximum short circuit current was found at 500nm thickness of absorber layer, but during simulation it has found that in case of Spiro-OmeTAD / $CH_3NH_3SnI_3$, the peak was observed at 600nm of thickness.

(a)

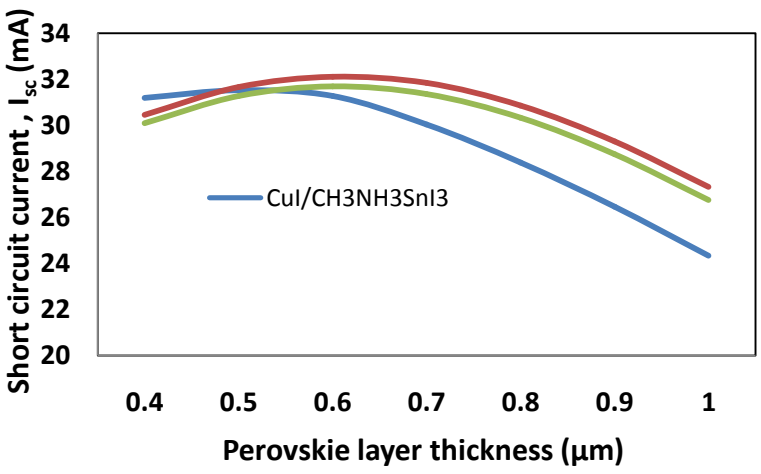

ISSN: 2411-9997

(b)

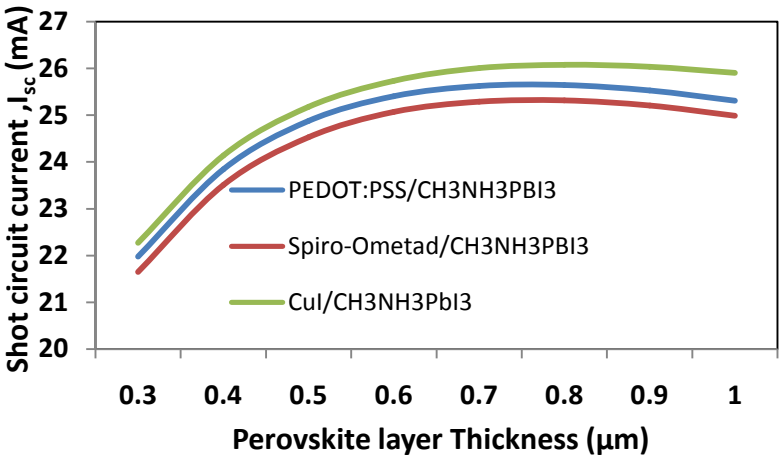

Fig.6: The short circuit current of a) Lead halide PVs b) Tin halide PVs with different HTM layer and with varying thickness of absorber.

In this research, the optimum thickness for the HTM layer has been investigated. The performance of the solar cell is hardly affected by the varying thicknesses of HTM. However, a sudden drop in performance was observed for varying thickness of Spiro-OmeTAD layer. Finally, a 3D graph has been plotted to understand the change of efficiency in terms of both varying thicknesses of absorber and HTM layer. This time, the parasitic resistance effect was neglected. The change in efficiency mainly depends on the perovskite layer thickness. The

(a)

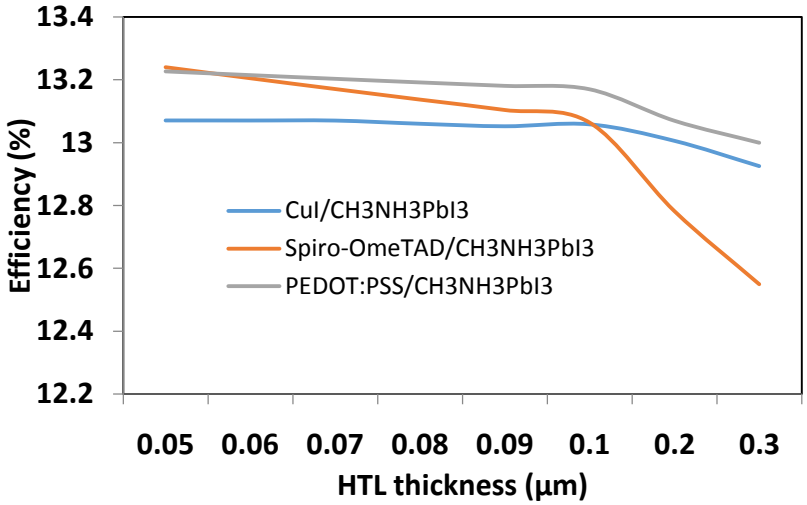

ISSN: 2411-9997

(b)

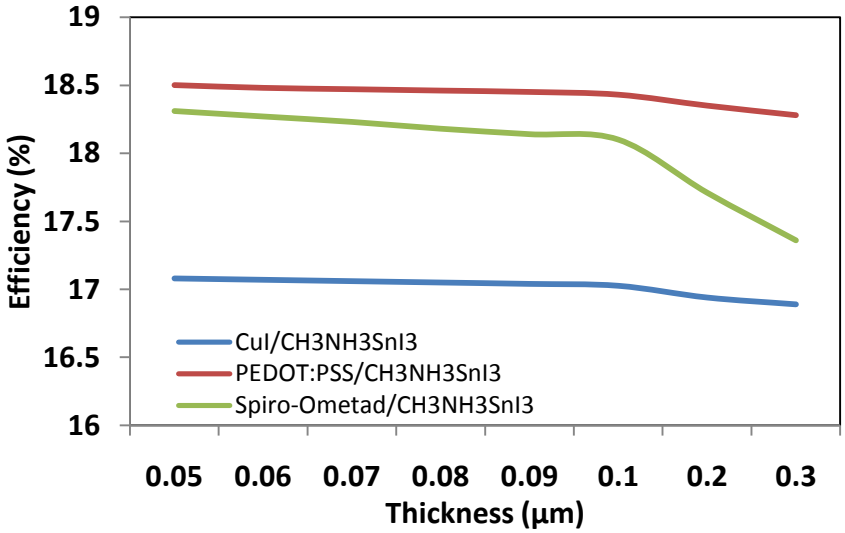

Fig. 7: The efficiency of a) Lead halide PVs b) Tin halide PVs with different HTM layer and with varying thickness of hole transport layer.

HTM layer thickness hardly affects efficiency. A large amount of data from the simulation was used to plot the graphs, and these graphs showed a pattern of how efficiency changes in perovskite structured solar cells with varying thickness of absorber and HTL. From these data and graphs, empirical equations are developed which can provide the result of efficiency combining the effect of both varying thicknesses of absorber and HTM layer.

a)

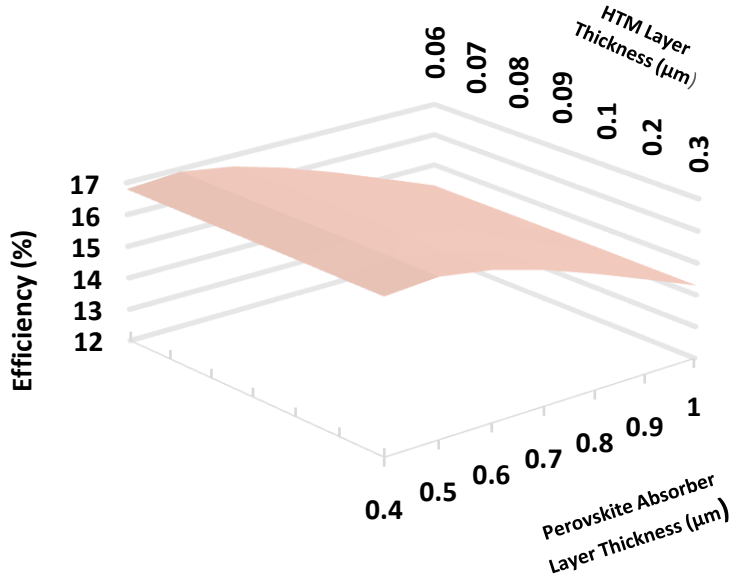

ISSN: 2411-9997

b)

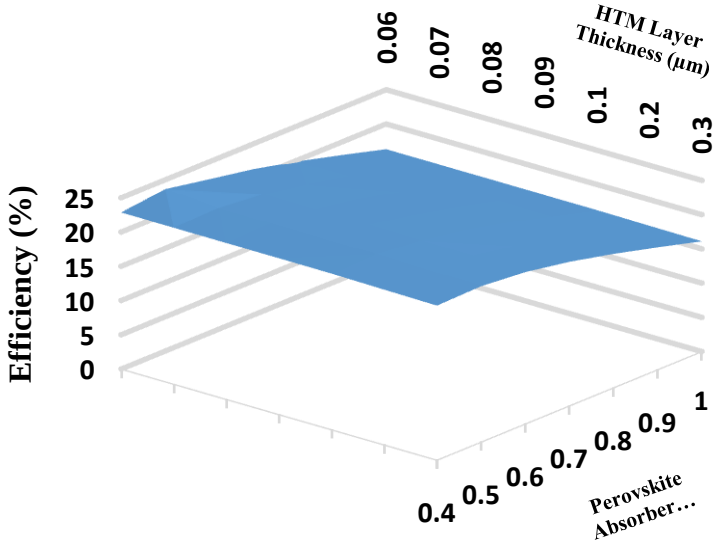

Fig. 8: The efficiency of a) lead halide & b) tin halide perovskite solar cell with varying thickness of absorber and PEDOT:PSS layer.

A function, f(x,y,z)=0 has been developed from the discrete simulating data where variables are defined by efficiency, the thickness of absorber and thickness of HTM. The efficiency mainly changes with varying thickness of perovskite solar cell, so an equation has been developed that can relate efficiency with varying thickness of the perovskite layer. After that, we observed how efficiency changes with varying thickness of the HTM layer. Fig. 8 helps us to have a good idea about the pattern of changing efficiency in terms of varying thickness HTL. The graphical demonstration (Fig. 8) is only for determining the efficiency of perovskite solar cell with varying thickness of absorber and PEDOT:PSS layer. Similarly, the authors also developed graph for CuI and Spiro-OmeTAD. From that observation, the authors calculated the deviation of efficiency with per µm change of thickness of HTL and generated another equation. Finally, two equations were combined to make an equation in an f (x,y,z)=0 form. In this paper, we presented six empirical equations for determining efficiency of PSC with varying thickness of absorber and HTM layer.

Table 5: Proposed equations for calculating efficiency of PSC with varying thickness of absorber and HTM layer.

Perovskite Solar Cell Structure	Equation for calculating efficiency F (x,y,z)=0
Spiro-OmeTAD/$CH_3NH_3PbI_3$	$z = 13.889x^3-33.75x^2+19.515x+2.3016y^2-3.7439y+12.858$
CuI/$CH_3NH_3PbI_3$	$z = - 29.735x^4+96.907x^3-117.99x^2+57.084x-0.4967y+6.4705$
PEDOT: PSS/$CH_3NH_3PbI_3$	$z = 14.722x^3-37.964x^2+26.063x-0.0876y+11.513$
Spiro-OmeTAD /$CH_3NH_3SnI_3$	$z = 27.778x^3-76.226x^2+52.935x+2.7307y^2-4.957y+11.9745$
CuI/$CH_3NH_3SnI_3$	$z = 27.5x^3-70.476x^2+43.713x+1.2086y^2-1.2423y+13.4282$
PEDOT: PSS/$CH_3NH_3SnI_3$	$z = 28.889x^3-79.774x^2+55.719x+1.3579y^2-1.5472y+11.686$

In above equations, x is for absorber layer thickness, y is for hole transport layer (HTM) thickness and z defines the efficiency.

4. Conclusion

The lead halide and tin halide perovskite solar cell with different hole transport layers has been simulated using SCAPS simulation package. The effect of various thicknesses of HTM layer and absorber layer on electrical characteristics of solar cell has also been investigated. The main findings are summarized as follows:

- Tin halide perovskite solar cell showed better efficiency than that of lead halide perovskite solar cell.

ISSN: 2411-9997

- An optimal thickness of tin and lead halide perovskite absorber layer is found to be 500nm and 400nm, respectively.
- The open-circuit voltage increases with the increase of absorber layer thickness vice versa for short circuit current.
- The efficiency slightly increases as the thickness of the hole transport layer decreases. However, a sudden drop in performance was observed for varying thicknesses of Spiro-OmeTAD layer.
- The PEDOT: PSS shows better performance than that of other three layers.
- The series and shunt resistance have a significant effect on the performance of the solar cell.

Acknowledgement

The authors would like to give acknowledgments to Marc Burgelman and his team at the University of Gent for the access of SCAPS-1D.

References

[1] H.J. Du, W.C. Wang and J. Z. Zhu, Chin. Phys. B 25, 108803 (2016).

[2] S. Kazim, M. K. Nazeeruddin, M. Gratzel and S. Ahmed, Angew53, 2812 – 2824 (2014).

[3] P. Umari, E. Mosconi and F. De Angelis, Sci. Rep. 4, 4467 (2015).

[4] A. Babayigit, D. D. Thanh, A. Etherirajan, J. Manca, M. Muller, H. Boyen and B. Conings, Sci Rep 6, 18721 (2016).

[5] Hao F., Stoumpos C.C., Cao D.H., Change R.P.H., Kanatzidis M.G. and N. Photon, J. Am. Chem. Soc. 136, 22, 8094-8099 (2014).

[6] Decock, Koen, Khelifi, Samira, Burgelman and Marc, Thi. Sol. Fil. 519, 7481 (2011).

[7] M. Burgelman, K. Decock, A. Niemegeers, J. Verschraegen and S. Degrave, Ver. 17 February (2016).

[8] J. Dong, Y. Zhao, J. Shi, H. Wei, J. Xiao, X. Xu, J. Luo, J. Xu, D. Li, Y. Luo and Q. Meng, Chem. Comm. 50, 13381 (2014).

[9] D. Y. Son, J. Im, H. Kim and N. Park, J. Phys. Chem. 118, 16567 (2014).

[10] X. Yang, T. Liu, Z. Li, B, Feng, S. Li, J. Duan, C. Ye, J. Zhang and H. Wang, App. Surf. Sci. 388, 89 (2016).

[11] M. Li ,P. Lin ,Y. Chiang ,C. Chan ,T. Guo and P.. Chen, Adv. Mater. Interfaces 2018, 1800882 (2018).

[12] M.Huangfu, Y. Shen, G. Zhu, K. Xu, M. Cao, F. Gu and L. Wang, App. Surf. Sci. 357, 2234 (2015).

[13] A. Uddin, M. A. Mahmud, N. K. Elumalai, D. Wang, M. Upama, M. Wright, K. Chan, F. Haque and C. Xu, Renew. Energy Environ. Sustain. 2, 7 (2017).

[14] M. Chen, M. Ju, H. Garces, A. Carl, L. Ono, Z. Hawash, Y. Zhang, T. Shen, Y. Qi, R. Grimm, D. Pacifici, X. Zeng, Y. Zhou and N. Padture, Nat. Commun. 10, 16 (2019).

[15] D. B. Mitzi, C. A. Feild, Z. Schlesinger and R. B. Laibowitz, J. Sol. State Chem. 114, 159 (1995).

[16] W. Li, H. Dong, L. Wang, N. Li, X. Guo, J. Li and Y. Qiu, J. Mater. Chem. A 2, 13587 (2014).

[17] Zhao X and Park N-G, Photonics 2, 1139 (2015).

[18] Zhang Y, Hu X, Chen L, Huang Z, Fu Q, Liu Y, Zhang L and Chen Y, Org. Electron. 30, 281 (2016).

[19] Correa-Baena J. P., Saliba M., Buonassisi T., Grätzel M., Abate A., Tress W. and Hagfeldt, Science, 358, 739 (2017).

[20] Tress and Wolfgang, Adv. Energ. Mat. 7, 1602358 (2017).

[21] Y. Zhao, H. Zhang, X. Ren, H. L. Zhu, Z. Huang, F. Ye, D. Ouyang, K. W. Cheah, K.Y. Jen and C. H. Choy, ACS Energ. Lett. 3, 2891 (2018).

[22] S. F. Hoefler, G. Trimmel and T. Rath, Monatsh Chem. 148, 795 (2017).

[23] S. Z. Haider, H. Anwar and M. Wang, Semicond. Sci. Tech. 33, 035001 (2018).

[24] H. Du, W. Wang and J. Zhu, Chin. Phys. B 25, 108803 (2016).

[25] F. Anwar, R. Mahbub, S. S. Satter and S. M. Ullah, Int. J. Photoenergy 2017, 9846310 (2017).

[26] U. Mandadapu1, S. V. Vedanayakam, K. Thyagarajan, M. R. Reddy and B. J. Babu, Int. J. Renew. Ener. Res. 7, 1603 (2017).

[27] B. M. Soucase, I. G. Pradas and K. R. Adhikari, In. Tech., ch.15 (2016).

[28] S. Sun, T. Salim, N. Mathews, M. Duchamp, C. Boothroyd, G. Xing, T. C. Sum and Y. M. Lam, Energ. Environ. Sci., 7, 399 (2014).

[29] J. H. Heo, H. J. Han, D. Kim, T. K. Ahn and S. H. Im, Energy Environ. Sci. 8, 1602 (2015).

[30] N. Ahn, D. Y. Son, I. Jang, S. M. Kang, M. Choi and N. Park, J. Am. Chem. Soc. 137, 8696 (2015).

[31] Li X., Yang J., Jiang Q., Chu W., Zhang D., Zhou Z. and Xin J., ACS Appl. Mat. 9, 41354 (2017).

[32] M. A. Green, Solar Cells - Operating Principles, Technology and System Application (Kensington, Australia: University of NSW) (1992).

ISSN: 2411-9997